

# REPORT DOCUMENTATION PAGE

*Form Approved*  
**OMB No. 074-0188**

Public reporting burden for this collection of information is estimated to average 1 hour per response, including the time for reviewing instructions, searching existing data sources, gathering and maintaining the data needed, and completing and reviewing this collection of information. Send comments regarding this burden estimate or any other aspect of this collection of information, including suggestions for reducing this burden to Washington Headquarters Services, Directorate for Information Operations and Reports, 1215 Jefferson Davis Highway, Suite 1204, Arlington, VA 22202-4302, and to the Office of Management and Budget, Paperwork Reduction Project (0704-0188), Washington, DC 20503

<b>1. AGENCY USE ONLY (Leave blank)</b>		<b>2. REPORT DATE</b> 1998	<b>3. REPORT TYPE AND DATES COVERED</b> Progress Report	
<b>4. TITLE AND SUBTITLE</b> Development of Laser-Based Sensors for VOC/NOx and Metals Emissions Monitoring, CP 1060-97 1998, Progress Report			<b>5. FUNDING NUMBERS</b> N/A	
<b>6. AUTHOR(S)</b> Scott E. Bisson, Meng-Dawn Cheng				
<b>7. PERFORMING ORGANIZATION NAME(S) AND ADDRESS(ES)</b>  Sandia National Laboratories Livermore, CA 94550			<b>8. PERFORMING ORGANIZATION REPORT NUMBER</b> N/A	
			Oak Ridge National Laboratory Oak Ridge, TN 37831-6407	
<b>9. SPONSORING / MONITORING AGENCY NAME(S) AND ADDRESS(ES)</b>  SERDP 901 North Stuart St. Suite 303 Arlington, VA 22203			<b>10. SPONSORING / MONITORING AGENCY REPORT NUMBER</b> N/A	
<b>11. SUPPLEMENTARY NOTES</b> The United States Government has a royalty-free license throughout the world in all copyrightable material contained herein. All other rights are reserved by the copyright owner.				
<b>12a. DISTRIBUTION / AVAILABILITY STATEMENT</b> Approved for public release: distribution is unlimited.				<b>12b. DISTRIBUTION CODE</b> A
<b>13. ABSTRACT (Maximum 200 Words)</b>				
<b>14. SUBJECT TERMS</b>				<b>15. NUMBER OF PAGES</b> 29
				<b>16. PRICE CODE</b> N/A
<b>17. SECURITY CLASSIFICATION OF REPORT</b>  unclass.	<b>18. SECURITY CLASSIFICATION OF THIS PAGE</b>  unclass.	<b>19. SECURITY CLASSIFICATION OF ABSTRACT</b>  unclass.		<b>20. LIMITATION OF ABSTRACT</b>  UL

**Development of Laser-Based Sensors for VOC/NO<sub>x</sub>  
and Metals Emissions Monitoring  
CP 1060-97  
1998 Progress Report**

**Scott E. Bisson  
Sandia National Laboratories  
Livermore CA, 94550**

**Meng-Dawn Cheng  
Oak Ridge National Laboratory  
Oak Ridge, Tennessee 37831-6407.**

JAN 1999

19990525 022

**Development of Laser-Based Sensors for VOC/NO<sub>x</sub>  
and Metals Emissions Monitoring  
CP 1060-97  
1998 Progress Report**

## **Introduction**

This project addresses the growing Department of Defense (DoD) and Department of Energy (DOE) needs to monitor air emissions in order to comply with more stringent regulatory pressures, such as the Clean Air Act Amendment (CAAA). Specifically, we are focused on the development of new technologies that will potentially increase the rapidity and degree of automation with which such measurements can be made. This project will culminate with the demonstration of two chemical sensing systems — one to measure gas-phase organic and inorganic molecular emissions, and the other to measure particulate and atomic metal emissions. The work is being done as a collaborative effort between Oak Ridge National Laboratory (ORNL) and Sandia National Laboratories (SNL). ORNL is responsible for the metal-emissions portion of the system; SNL is responsible for the molecular gas-phase portion.

The gas-phase portion of the system utilizes infrared (IR) absorption spectroscopy to detect analytes of interest. The IR absorption spectra of air samples are determined using laser photoacoustic spectroscopy (PAS), in which a sensitive microphone is used to sense the acoustic wave produced by laser energy deposited in the gas-phase molecules. PAS can detect absorptions as small as 1 part in  $10^7$ , allowing detection of many species at the high ppt to ppb levels. A schematic of the prototype photoacoustic spectrometer is shown in figure 1. The major components of this system are the Nd:YAG pump laser, the tunable infrared OPO, photoacoustic cell and a laptop computer. Our approach to PAS differs from earlier work in its use of a new development in tunable IR lasers. The new technology, termed quasi-phasesmatching (QPM), makes it possible to develop nonlinear optical materials whose performance exceeds that of conventional crystals by over an order of magnitude. The idea of quasi-phase matching is not new; it dates back to 1962 but methods for manufacturing QPM materials had not yet been developed. Within the last 5 years however, methods for manufacturing QPM materials based on lithium niobate ( $\text{LiNbO}_3$ ) have been developed using photolithographic techniques borrowed from the semiconductor industry. Quasi-phasesmatched lithium niobate differs from bulk lithium niobate in that the optical axis of the crystal is periodically reversed or poled. When pumped by the fundamental of an Nd:YAG laser, periodically-poled lithium niobate (PPLN) offers the possibility of broad spectral coverage over the mid-infrared region with unprecedented

performance. Through a nonlinear coupling between the pump laser and the PPLN crystal, the pump light is split into two *tunable* wavelengths (termed the signal and idler) which are determined by the period of the domain reversal of the crystal and the pump wavelength. By manufacturing PPLN crystals with varying periods broad tuning can be achieved.

The use of periodically-poled lithium niobate (PPLN) in laser devices is growing quickly. PPLN's high nonlinearity, long interaction length, and the ability to *engineer* the poled structure (and hence the spectral properties) using a photolithographic mask make it an attractive nonlinear material for many applications. By controlling the poled regions through photolithography, a single crystal can be engineered for many different frequency

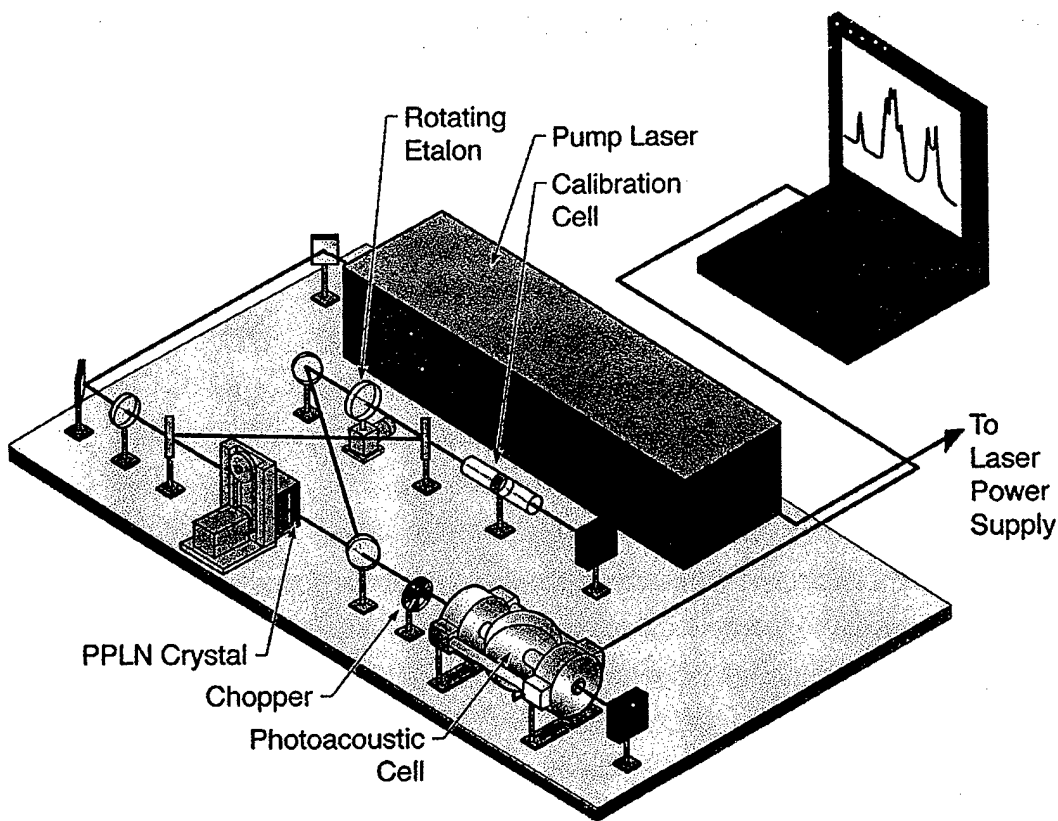


Figure 1. Schematic of the prototype breadboard spectrometer.

mixing applications. Currently crystals with as many as eight discrete poled regions or with continuously varying periods are commercially available. The high nonlinearity and long interaction length brings the efficiency of many nonlinear frequency conversion techniques to the point where they are suitable for spectroscopy using small lasers. For example, recent work in our laboratory and other labs have demonstrated generation of greater than 30  $\mu$ Watts of power through difference frequency (DFG) conversion using

two 0.5 W diode lasers.<sup>1,2</sup> This amount of DFG power is enough for techniques such as wavelength modulation and frequency modulation spectroscopy. Another application of PPLN's high nonlinearity and long interaction length is the successful demonstration of a cw singly resonant optical parametric oscillator (SRO) pumped with the relatively low threshold of 3 W.<sup>3</sup> Pump powers as low as 800 mW have been used to pump a PPLN SRO when both the pump and signal are resonated.<sup>4</sup> The use of PPLN in OPOs is described in detail in ref. 5.

We are employing PPLN to fabricate a compact IR optical parametric oscillator (OPO — a type of laser) that allows continuous breadth of tuning (1.3-4.5  $\mu\text{m}$ ) and output power (~200 mW) that were not attainable in a fieldable package in the past. High output power is required to attain the PAS sensitivities required in regulatory applications such as ambient air monitoring or stack monitoring. Continuous tuning reduces ambiguity in spectral identification and discrimination against background materials. Operation in the 1.3 to 4.5  $\mu\text{m}$  range allows detection of many organic effluents, as it encompasses the range in which C-H bonds absorb. The primary existing competitors to this technology are (1) the CO<sub>2</sub> laser, which is only discretely tunable over ~50 lines in the 9-11  $\mu\text{m}$  spectral range, and (2) OPO's based on conventional nonlinear materials, which are tabletop-sized systems that are not conducive to operation in a field environment.

The portion of the system that is devoted to metals monitoring employs laser-induced breakdown spectroscopy (LIBS) (also referred to as laser -induced plasma spectroscopy (LIPS)). These are established methods of atomic detection that have been demonstrated to sense sub-ppm levels of many elements such as Hg, Pb, Ni, and Cr. Our work can be distinguished from existing technology in its focus on miniaturization and its exploration of the viability of LIBS as a continuous emission monitor (CEM). This is being accomplished by exploiting many advanced opto-electronics, microelectronics, and laser components that have been developed at the ORNL as well as other Federally Funded Research and Development Centers.

The physical mechanism of LIBS detection is that the laser introduces a shot (or multiple shots) of coherent light energy to a small volume air sample that consists of gas and aerosols. This shot vaporizes the material in the volume, which then contains high density of electrons at high temperature as a result of the laser bombardment. The metal atoms excited by the laser emit light at characteristic wavelengths that can be measured by solid-state detectors. The detection process takes place on a microsecond timescale and provides the ability to measure the spatial and time-resolved distribution of metal emissions in real time and in-situ with no sample preparation requirement. LIBS is also ideally suited

to analyze samples in remotely accessible or hazardous environments without handling the sample or exposing the analyst to hazards.

The analytical principle of the laser-induced breakdown technique has been known since the 70's. There has been work done using LIBS for detecting metals in media such as aerosols, liquids, soils, and gases. Most of this work was done using large lasers such as the Nd:YAG and complicated and delicate optical and electronic components, which also weigh several hundred pounds, making the system unsuitable for field operation. Earlier LIBS systems used a box car analyzer to perform spectroscopic work, recent systems used polychromators, which are also bulkier and heavy. Although the laboratory systems have successfully demonstrated the LIBS principle for metal measurement, it requires a considerable effort to develop a LIBS system for field measurement (i.e., in making the system compact, light-weight, and rugged). Using advances made in micro-manufacturing, solid-state laser development, and associated optical hardware (i.e., spectrometers, fiber optics), there is a good possibility to develop a new generation of LIBS system for measuring atmospheric metals. ORNL has developed a prototype low-cost *micro* -spectrometer for which patents are pending. This monolithic micro-sensor device was developed by an extremely tight fabrication tolerance alignment-free tooling system. The device occupies only about six cubic centimeters in volume, has a 1024-element linear CCD array, and is well-suited for the portable LIBS system. This, coupled with recent advances in micro-chip lasers offer the promise of an extremely compact, low-cost LIBS sensor.

### **Project Information**

This project is a three-year effort funded jointly at SNL and ORNL. This report describes work accomplished during the second year of this project from the period from February, 1998 (when funding was received at the laboratories) thru December, 1998. Support for this project was also leveraged under an MOU with Coherent Laser Group (CLG) of Santa Clara CA. The total SERDP funding received during this period was \$1040K (\$580K to ORNL; \$460K to SNL). The points of contact for Sandia and Oak Ridge are:

Scott E. Bisson  
Mail Stop 9051  
Sandia National Laboratories  
7011 East Ave.  
Livermore CA, 94550  
Ph.: (925) 294-2467  
Fax: (925) 294-2276  
Email [sebisso@sandia.gov](mailto:sebisso@sandia.gov)

Meng-Dawn Cheng  
Environmental Sciences Division  
Oak Ridge National Laboratory  
Building 1505, RM 350 MS 6407  
Oak Ridge, Tennessee 37831-6407.  
Ph.: (423) 241-5918  
Fax: (423) 574-4665  
Email: chengmd@ornl.gov

### **Progress during FY 1997**

The remainder of this report describes progress made during the February - December, 1998 time period. The report is divided into two sections; the first describing the gas-phase molecular detection component; the latter describing the metals component.

### **VOC-NO<sub>x</sub> Detection Channel**

During the second year of this project our efforts were focused primarily on two tasks: first, establishing broad tunability of the PPLN OPO and second, evaluating photoacoustic cell designs for sensitivity and noise. We have also automated much of the laser tuning and data acquisition. The system components such as the pump laser, PPLN OPO and photoacoustic cell have been integrated onto a single breadboard.

For the laser, demonstrating broad tunability was key to the success of the project. We have pursued two tuning strategies: continuous tuning and mod-hop tuning. While both tuning strategies were successful we have selected mod-hop tuning due to its simplicity, lower risk and robustness. In both cases the OPO cavity was based on the proven design developed by Bosenberg et al.<sup>3</sup> This design was used in another OPO developed in our laboratory under funding from the Gas Research Institute (GRI) giving us confidence in its performance.

In the continuous tuning approach our goal was to obtain continuous tuning over 1-2 cm<sup>-1</sup> segments with broad tuning over several hundred wavenumbers. These scans would then be joined in software to produce a continuous spectrum. The challenge is to synchronize the scanning of intra-cavity tuning elements and also to actively stabilize the laser frequency against perturbations such as vibration and air currents. This method is presently used in commercial tunable cw dye lasers. Coherent Laser Group of Santa Clara, CA has considerable experience in the development of tunable laser systems and we have signed an MOU with Coherent to acquire some of their lock-loop and frequency scanning technology. Under this collaboration we have obtained one of their tunable OPOs for evaluation. Coherent has also expressed interest in commercializing the photoacoustic spectrometer.

The mode-hop tuned system tuned in discrete steps on the order of  $.02\text{-}.1\text{ cm}^{-1}$ , depending on how many cavity modes were jumped. The smallest step size was limited by the optical length of the cavity which for this system was approximately 580 MHz. For most atmospherically broadened species which have a linewidths on the order of a few GHz this mode spacing is small enough to resolve most spectral features. This method of tuning is attractive in that it is simple, employing only an intra-cavity etalon and no lock-loops or feedback circuits.

We have also made substantial progress on the design of the photoacoustic cell. Under a collaboration with Dr. Jos Oomens from the Catholic University of Nijmegen, The Netherlands, we have tested an alternate photoacoustic cell design with the PPLN OPO. Using this cell we have achieved measurement sensitivities on the order of 10 ppb for ethane and pentane. This design will soon be incorporated into our photoacoustic spectrometer. In addition to demonstrating broad tunability we have also spent considerable effort on the stabilization (both passive and active), thermal management and computer control.

## **Laser**

### **Source Requirements**

The choice of photoacoustic spectroscopy as the detection method and the need to detect a broad range of species places certain requirements on the laser. First, to be sensitive it should be cw and capable of an output of a few hundred mWatts or more and second, broad tunability is essential. Other obvious requirements are compactness, high efficiency and ruggedness for field operation. In addition to broad tunability, the optimum wavelength range is in the  $3\text{-}5\mu\text{m}$  range where many functional groups such as C-H absorb or in the  $8\text{-}12\mu\text{m}$  range where atmospheric transmission is good and absorptions are strong. These requirements are best satisfied through the use of OPO based on PPLN. The high nonlinearity, long interaction length, and the ability to engineer the poled structure using a photolithographic mask make PPLN an attractive nonlinear material for many applications. The high nonlinearity and long interaction length brings the efficiency of many nonlinear frequency conversion techniques to the point where they are suitable for spectroscopy using small lasers. Under funding from the Gas Research Institute (GRI) and SERDP we have demonstrated efficient cw, single frequency operation of a PPLN OPO. Outputs as high as several hundred milliwatts with several hundred wavenumbers of coarse tuning in the  $3\mu\text{m}$  region have been routinely obtained. While coarse tuning of a PPLN OPO over a broad spectral range has been demonstrated fine tuning over a broad spectral range has not yet been demonstrated. Fine tuning is essential for any spectroscopic

or chemical sensing application. During the second year of this project we have focused on the fine tuning capability of the OPO and have made significant progress towards this goal. The following describes the laser system and our tuning approaches.

### Laser System

A schematic of the laser system is shown in figure 2. The basic configuration of the OPO was a bow-tie ring geometry employing a fan type PPLN crystal. This design was discussed in a previous paper.<sup>6</sup> The ring configuration provided better frequency stability, single mode operation and more space for intra-cavity tuning elements than a linear cavity. The OPO cavity was formed by two concave mirrors,  $R=10\text{cm}$ , with the PPLN crystal in between and two flat mirrors forming the outside leg of the ring. The curved mirrors were coated on both sides for high transmission ( $>98\%$ ) of the pump beam at  $1.064\ \mu\text{m}$  and for high reflectivity ( $>99.5\%$ ) on the curved surfaces at  $1.57\ \mu\text{m}$ .

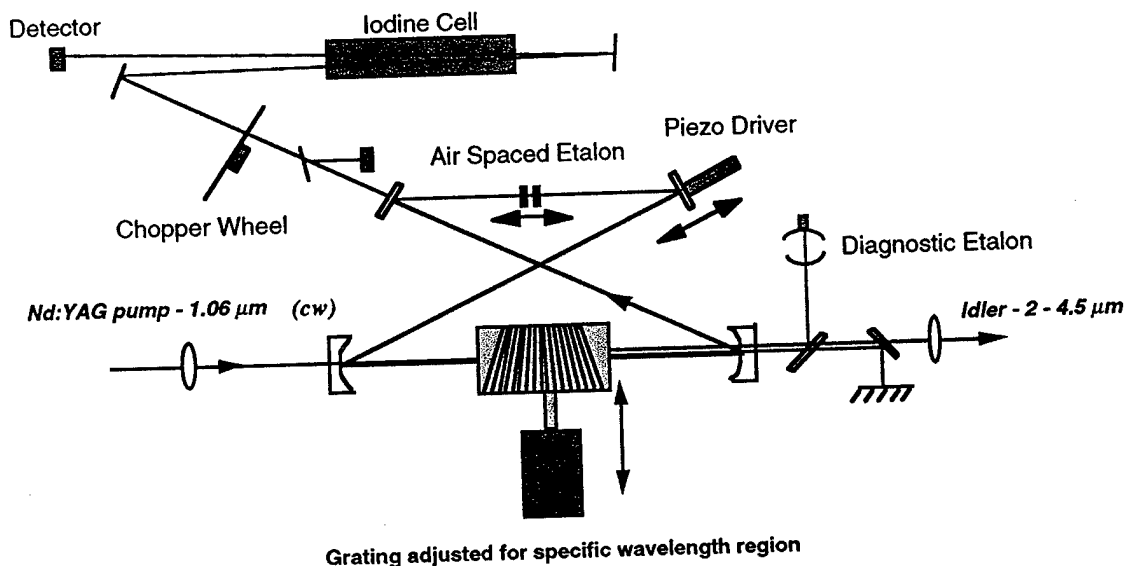


Figure 2. Schematic diagram of the cw ring OPO used in this work.

The reflectivity at  $3.0\ \mu\text{m}$  was made as low as possible to avoid idler feedback and to couple as much  $3.0\ \mu\text{m}$  light out of the cavity as possible. We have found that with the ring geometry the oscillating mode tends to operate *single* mode or single frequency even without intra-cavity tuning elements. This was not the case with a linear resonator where random mode hopping and multi-mode operation were frequent. In this cavity we resonate the  $1.5\ \mu\text{m}$  signal wave and couple out the  $3\ \mu\text{m}$  idler wave. It is preferable to resonate the

3 $\mu\text{m}$  idler wave but due to mirror coating considerations it is easier to resonate the 1.5 $\mu\text{m}$  signal wave.

The OPO was pumped by a cw, single-logitudinal-mode, diode-pumped 6 watt Nd:Vanadate laser manufactured by Coherent Inc. Single mode operation of the pump laser was necessary for achieving single frequency operation at 3.0  $\mu\text{m}$  since the idler spectrum mirrored that of the pump spectrum. A multi-mode pump could be used if the idler wave were resonated inside the OPO cavity instead of the signal wave. However, as discussed above this is difficult due to mirror coating considerations. The pump beam was focused to approximately 100 $\mu\text{m}$  in diameter (intensity 10-90% power points) inside the PPLN crystal. The oscillation threshold was approximately 3 watts and when pumped at full power (6.5watts) a pump depletion of 85-90% could be achieved.

The PPLN crystal was of the fan type as shown in figure 3 with periods ranging from 29.3  $\mu\text{m}$  to 30.1  $\mu\text{m}$ . This yielded a coarse tuning range of approximately 350  $\text{cm}^{-1}$  from 1.53 to 1.62  $\mu\text{m}$  in the signal and 3.1  $\mu\text{m}$  to 3.5  $\mu\text{m}$  in the idler. The crystal dimensions were 50 mm long, 20 mm wide, and 0.5 mm thick. A 1 $^\circ$  wedge between the input and output facets helped to eliminate idler feedback in the OPO. The faces of the PPLN crystal were anti-reflection coated at both 1.064  $\mu\text{m}$  and also at 1.57  $\mu\text{m}$ . To avoid

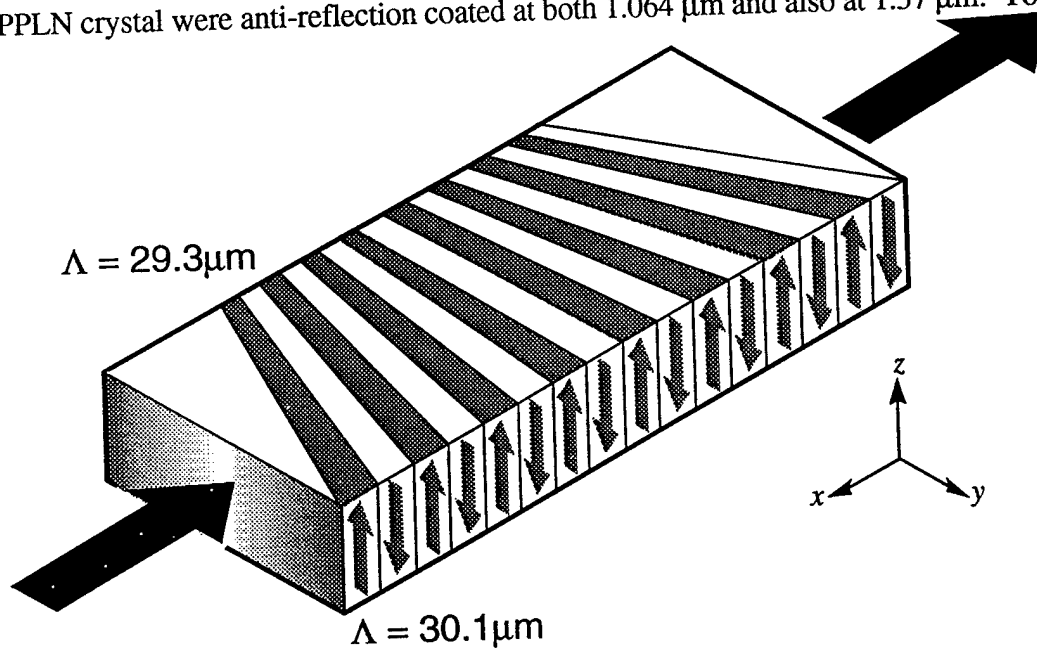


Figure 3. Exaggerated view of the fan-out pattern on the PPLN crystal. Arrows within the crystal indicate the poling direction. For the OPO, the pump, signal, and idler beams are polarized along the crystallographic z-axis (as indicated by the coordinates in the figure), and they propagate along the x-axis (as indicated by the large arrows entering and leaving the crystal), sampling only one periodicity.

photorefractive damage, the PPLN crystal was placed in an oven and heated to approximately 140 C during operation. We have recently designed a highly efficient oven which isolates the OPO cavity from thermal air currents and which requires very low power. This oven design holds the PPLN temperature to within 0.1C and has substantially improved the passive frequency stability of the OPO.

### Tuning Strategies

We are pursuing two tuning strategies for the OPO; mode-hop tuning and continuous tuning. In the mode-hop tuning approach, an intra-cavity etalon was used to control which longitudinal mode or frequency the OPO oscillates. The basic cavity configuration was similar to the continuous tuning approach as shown in figure 1 except that the air-spaced etalon was replaced with a 400 $\mu$ m solid YAG etalon. For mode-hop tuning, the etalon was rotated in discrete steps which yielded discrete frequency steps on the order of .02-.1  $\text{cm}^{-1}$ , depending on the number of cavity modes jumped. The required finesse of the etalon or spectral rejection is actually quite low on the order of a few percent or so. The etalon which worked best in our setup was a 400  $\mu$ m thick uncoated YAG substrate. The tuning range of the etalon was limited by walkoff losses within the etalon and also by the gain bandwidth of the PPLN crystal. These factors combined to give a mode-hop tuning range of approximately 4  $\text{cm}^{-1}$ . Although it may appear that an arbitrarily small frequency step can be obtained by a small rotation of the etalon this was not the case. The step size was limited by the optical length of the cavity or the free spectral range which for this system was approximately 580 Mhz. For most atmospherically broadened species which have a linewidths on the order of a few GHz this mode spacing is small enough to resolve most spectral features. To achieve scans larger than 4  $\text{cm}^{-1}$  the PPLN crystal was translated approximately .04 mm which moved the OPO gain peak approximately 4  $\text{cm}^{-1}$ . Figure 4 shows several scans obtained by mode-hop tuning of the OPO. This method of tuning is attractive in that it is simple, employing only an intra-cavity etalon and no lock-loops or feedback circuits.

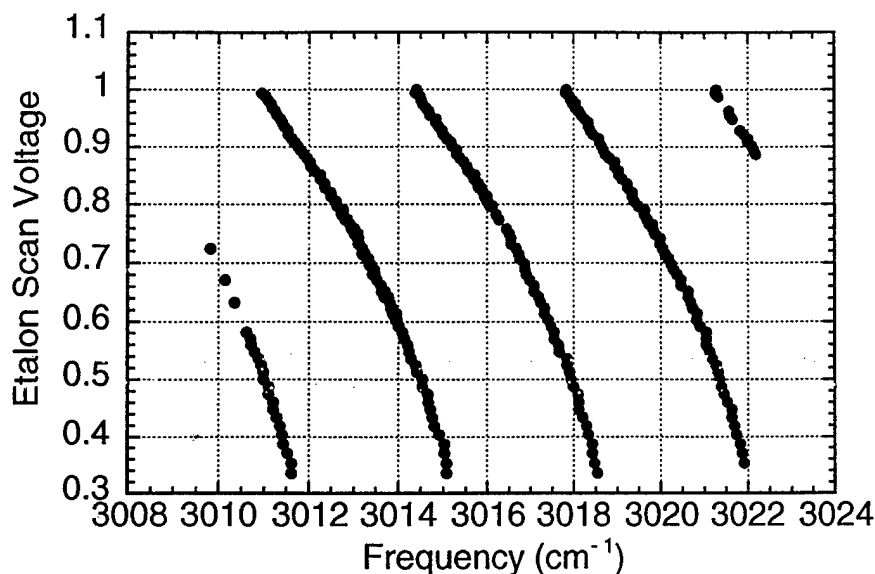


Figure 4. Plot showing mode-hop tuning of the OPO. For mode-hop tuning, the etalon was rotated which tuned the laser over approximately  $4 \text{ cm}^{-1}$ . Tuning outside of this range requires translating the PPLN crystal to a new grating period. This produces the family of curves above.

For continuous tuning it is necessary to tune the OPO cavity mode synchronously with the etalon. Our goal was to demonstrate approximately  $1\text{-}2 \text{ cm}^{-1}$  of continuous tuning using this approach. Figure 2 shows the cavity configuration used for continuous tuning. Here, an air spaced etalon was used to confine the cavity mode or oscillation frequency. An air-spaced etalon has the advantage in that it is tuned by varying the spacing of the air gap and not by rotating, thus eliminating the variable walk-off losses. To achieve continuous tuning the cavity length is varied either with an internal element such as a rotating Brewster plate or more simply by translating a cavity mirror. We have chosen the latter. This eliminates the need for inserting a lossy internal cavity element and also is somewhat simpler. The drawback is that large translations on the order of  $40 \mu\text{m}$  are required. The most reliable method of translation on this scale is through the use of piezo-electric transducers. The cavity used in our setup used a multiple stack piezo which was capable of translations on the order of  $40 \mu\text{m}$ . The effective tuning was actually twice this since the optical cavity length changes by twice the translation amount. The goal was to demonstrate approximately  $1\text{-}2 \text{ cm}^{-1}$  of continuous tuning.

As the cavity length is changed, i.e. shortened, the cavity modes shift to shorter wavelengths. The etalon is then slaved by a lock-loop to the peak of a cavity mode and

tracks the cavity mode as the cavity is tuned. The challenge is to keep the etalon locked to the cavity mode as the cavity length is tuned. There are many perturbations which can disrupt the tuning process such as air currents inside the cavity caused by the PPLN oven. Rapid thermal changes in the PPLN crystal can change the effective optical length of the cavity. Some of the perturbations such as convection currents generated by the PPLN oven can be controlled by isolating the oven. Others, like the rapid thermal fluctuations inside the PPLN (caused in part by absorption of  $3\mu\text{m}$  light in the crystal) crystal cannot be controlled. If the perturbations occur too rapidly, ie, outside the bandwidth of the lock loop or if the perturbation was too large then the OPO would mode hop. To keep the insertion losses low the etalon was of relatively low finesse making the cavity more susceptible to mode hops. The etalon also had to be of low mass so that the loop response frequency would be high.

While the continuous tuning method described here has been used quite successfully on tunable dye lasers<sup>7</sup> the application to tunable OPOs possess many different challenges. In particular, we have observed that although the cavity mirrors are designed to transmit the  $3.0\ \mu\text{m}$  light there is enough feedback to cause a double resonance effect. Doubly resonant OPOs are in general very unstable. As the cavity length was tuned in our system the  $1.5\ \mu\text{m}$  light would tune continuously and the  $3.0\ \mu\text{m}$  light would tune continuously in the opposite direction. However, there were occasions when the  $3.0\ \mu\text{m}$  light was slightly resonant in the cavity which raised the intra-cavity  $3\ \mu\text{m}$  power. This in turn raised the temperature of the PPLN crystal which effectively changed the optical length causing the laser to tune uncontrollably. To mitigate this problem, we have purchased optics which were more effective in rejecting intra-cavity  $3.0\ \mu\text{m}$  light. Unfortunately, the intra-cavity etalon was somewhat lossy and we have not fully tested this method of tuning with our OPO. We have however verified the performance of the etalon in another tunable OPO being developed at Coherent Laser Group in Santa Clara, CA. This system had the advantage of a higher pump power (10 watts) so the cavity could tolerate a higher intra-cavity loss.

As part of our commercialization goal and also to facilitate a more rapid development of the tunable laser source we have signed an MOU with Coherent Laser Group. Coherent has a long history in the development of continuously tunable visible and near IR lasers and is also presently developing technology that would be useful for the tunable laser system being developed under SERDP support. Under the terms of the MOU, Sandia will acquire key lock loop and scanning technology. In addition, we will acquire broad band optics which should extend the broad tuning range of the laser. The lock loop technology developed at Coherent has already been tested with our air-spaced etalon and they have

demonstrated over  $2 \text{ cm}^{-1}$  of continuous tuning with this system. Coherent has expressed great interest in manufacturing both the laser and also the sensor. We hope that following the MOU a CRADA would be put in place to continue development of the sensor.

### Photoacoustic Spectroscopy

The wide range of physical properties of the gaseous pollutants defined under the Clean Air Act Amendment poses a formidable detection challenge. Photoacoustic spectroscopy is an ideal method of detection since it is sensitive and capable of detecting species with both broad and narrow spectral features. Photoacoustic spectroscopy operates by monitoring the heat deposited in a volume containing the gas of interest while scanning the input wavelength. This is in contrast to traditional spectroscopic techniques which monitor the *transmitted* or absorbed laser light as a function of wavelength. Many absorption techniques such as frequency modulation and wavelength modulation spectroscopy are derivative techniques and in general are sensitive only to small molecules with well defined spectral features (large derivatives) but are not amenable to large molecules with broad spectral features. The difference between the spectra of a large molecule such as toluene and a small molecule such as  $\text{NO}_2$  are illustrated in figure 5. Only photoacoustic spectroscopy has all of the attributes required for a CEM monitor. Another advantage is that under normal operating conditions it is a linear technique thus facilitating easy analysis.

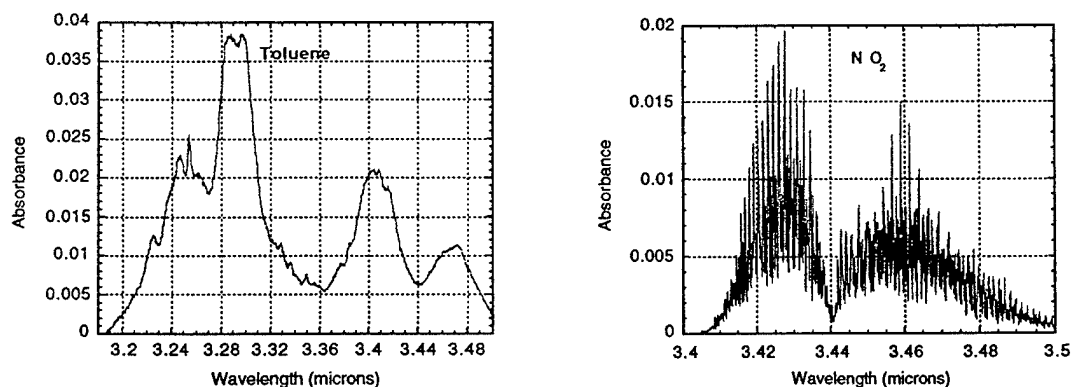


Figure 5. Comparison of absorption spectra for a large molecule such as toluene and a small molecule such as  $\text{NO}_2$ . Photoacoustic spectroscopy is ideal for the detection of species with both broad and narrow spectral features.

The heat deposited in photoacoustic spectroscopy is monitored not by the temperature but by the acoustic pressure wave that is created by the expanding hot gas. A simple hearing aid microphone is sufficient for this purpose. The technique can be employed in either pulsed or cw modes. In the pulsed mode, a pulsed laser is directed into a cell containing the gas to be monitored and the ballistic pressure pulse is then detected. For continuous wave (cw) operation, a cw laser beam is chopped (usually at a few kHz) and the chopped acoustic frequency is detected, not individual pulses. We have explored the pulsed mode of operation in our laboratory and found that while pulsed operation was sensitive the PPLN laser technology was actually more mature for cw operation. Therefore, this is the path that we have chosen. CW operation does however place some difficult requirements on the laser. In general, to achieve high sensitivity it is desirable to have an average power of a watt or greater. High intensity on the other hand is undesirable as the spectral resolution can be degraded. These seemingly mutually exclusive requirements can be met through the use of an acoustically resonant cell. Here the acoustic signal is resonantly enhanced by using an acoustically resonant cell. This simultaneously reduces the required excitation power and also reduces the potential for spectral power broadening.

### Cell Design

There are several criteria that need to be considered in the design of a photoacoustic cell for a field portable sensor. For cw operation the cell should be acoustically resonant to enhance sensitivity and the windows should be isolated from the main resonant chamber. Furthermore, for rapid analysis the volume should be small so that the gas volume can be exchanged rapidly. A large mass is also desirable to dampen external acoustic noise. The strength of the photoacoustic signal depends on a number of factors: the overlap of the laser beam and the acoustic mode being excited, the intensity of the laser beam, the excitation or chopping frequency, the volume and Q of the cell and the absorption properties of the gas.

Figure 6 illustrates one of the resonant acoustic cell designs we have tested. In this design a chopped cw laser beam entered the cell through an acoustic filter and then into the main acoustic chamber. The acoustic filters were used to reduce window noise (due to absorption of the laser beam) from reaching the microphone. Furthermore, the main acoustic chamber is mounted at an angle to the laser beam. This is so that the laser beam would be coupled into the cell at a node of the acoustic cell thus further reducing the potential for the coupling of outside noise into the microphone. This idea was first demonstrated by Gerlach and Amer<sup>8</sup> and is the basis for the approach used here. The cell design in figure 6 is a variant of this design and was developed by Meyer and Sigrist.<sup>9</sup>

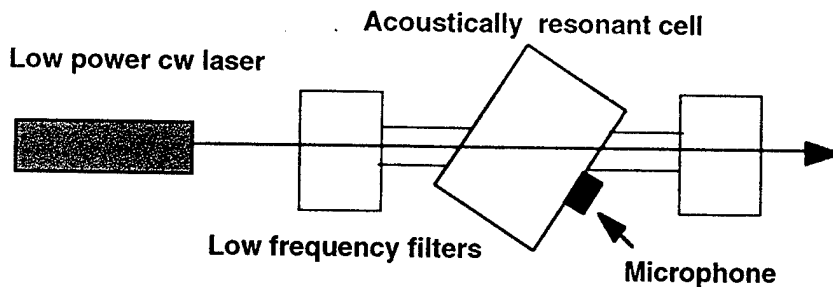


Figure 6. Design for an acoustically resonant cell. The filters at the input and output of the cell are used to reduce the coupling of window noise into the main acoustic chamber. The main acoustic chamber is mounted at an angle with respect to the main beam and at an acoustic node to reduce coupling of noise.

This cell has a resonant frequency of 2675 Hz and a Q of approximately 200. The main resonant chamber is circular with dimensions of 6.54 cm  $\times$  15.56 cm (diameter) yielding a volume of 1243 cm<sup>3</sup>. We have found that while the cell had a high Q and was therefore quite sensitive it was prone to picking up background noise. The background noise had three main components: a random component, a coherent component proportional to the laser power and a coherent component that was independent of laser power. The main source of noise was coherent noise generated from the chopper wheel. This noise has been reduced by evacuating the air inside the chopper wheel. Figure 7 shows an example of the spectrum of the Q-branch of methane taken with this cell using the mode-hop tuned PPLN source.

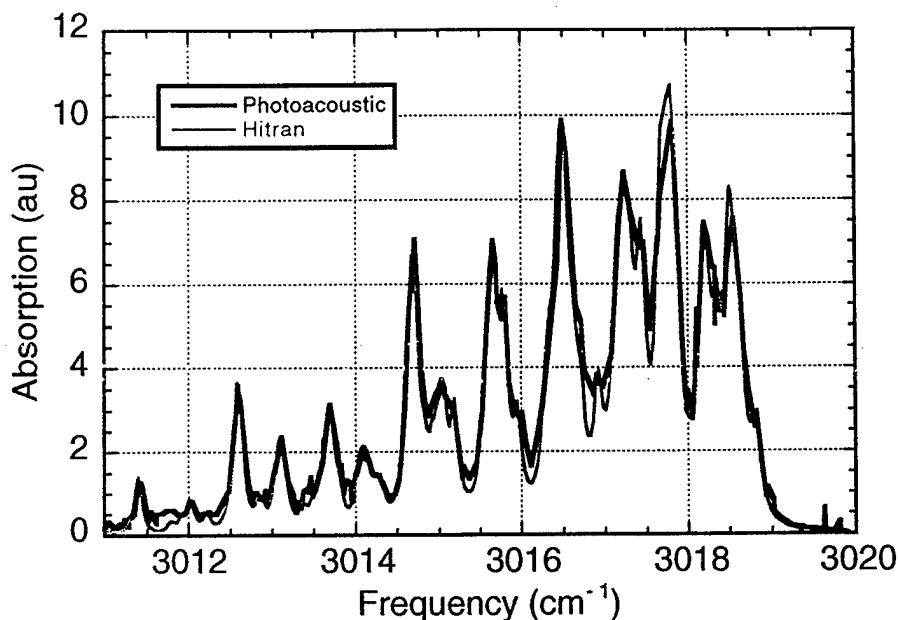


Figure 7. Spectrum of the Q-branch of methane acquired with the mode-hop tuned PPLN laser source and resonant photoacoustic cell. This spectra compares well with a theoretical spectrum from the Hitran database and illustrates the high quality data and spectral resolution that can be achieved with a mode-hop tuned source.

Under a collaboration with Dr. Jos Oomens of the Catholic University of Nijmegen, The Netherlands, we have experimented with an alternate acoustic cell design. While this design was similar to our original design in that it had a main acoustic chamber and acoustice traps to reduce window noise there were some very important differences. The volume of this cell was considerably smaller ( $15 \text{ cm} \times 1.78 \text{ mm}$  diameter) which allowed for rapid exchange of gas. Moreover, since the acoustic excitation amplitude is inversely proportional to the volume the excitation amplitude was considerably greater. The excitation amplitude is also inversely proportional to the resonant frequency squared and for this cell the resonant frequency was approximately 1600 Hz, which was considerably lower than the resonant frequency of our first cell (2675 Hz). Finally, the cell was much more massive which greatly reduced the coupling of external acoustic noise into the cell. Thus, even though the Q of this cell was much lower than our original design the combination of a larger mass, smaller volume and a lower resonant frequency made for a more sensitive cell. This cell was extremely sensitive and has even been used to detect the respiration of cockroach and even a gnat.<sup>10,11</sup> The lower Q ( $\sim 10$ ) of this cell is also

desirable in a field environment since the cell temperature can change thus shifting the cell resonant frequency and response. Using this cell with the PPLN laser source we have made sensitivity measurements of ethane and pentane. These measurements were made with the gas diluted in pure nitrogen and at atmospheric pressure. These data are shown in figures 7 and 8. For ethane, we achieved an extrapolated sensitivity of approximately 15 ppb and for pentane the extrapolated sensitivity was approximately 22 ppb.

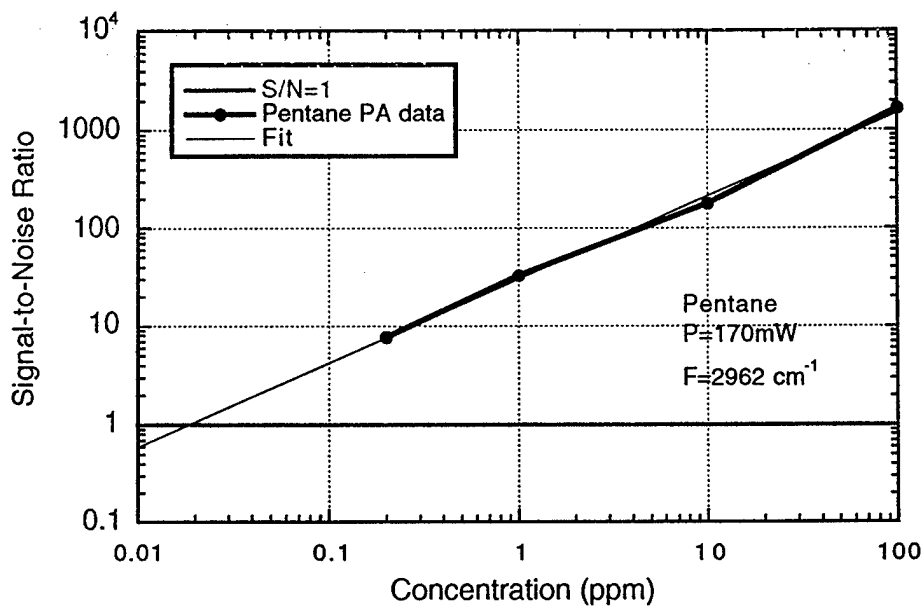


Figure 7. Photoacoustic sensitivity measurement of pentane.

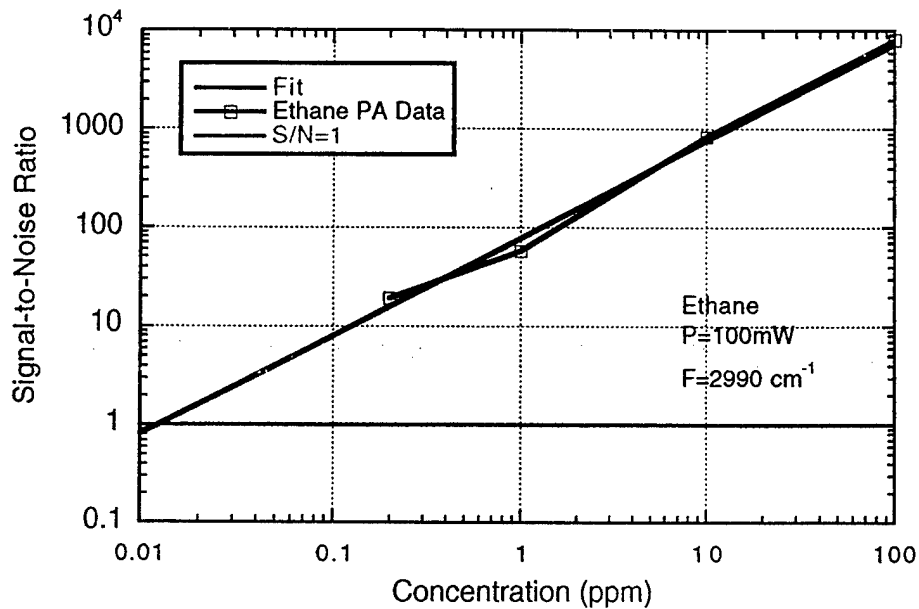


Figure 8. Photoacoustic sensitivity measurement of ethane.

### Spectrometer

Figure 9 shows a photograph of the photoacoustic system. The major components of this system are the pump laser ( VERDI manufactured by Coherent Inc) the PPLN OPO, the photoacoustic cell and the data acquisition, control and analysis computer (IBM Think Pad). The components were mounted on an optical breadboard approximately 3 ft by 2 ft which permitted easy access to hardware and also easy modification. The system is stand alone except for the requirement of 120V 15A electrical service. No cooling water was required for the laser. All data acquisition, control and analysis were near real-time thus eliminating the need for post analysis.

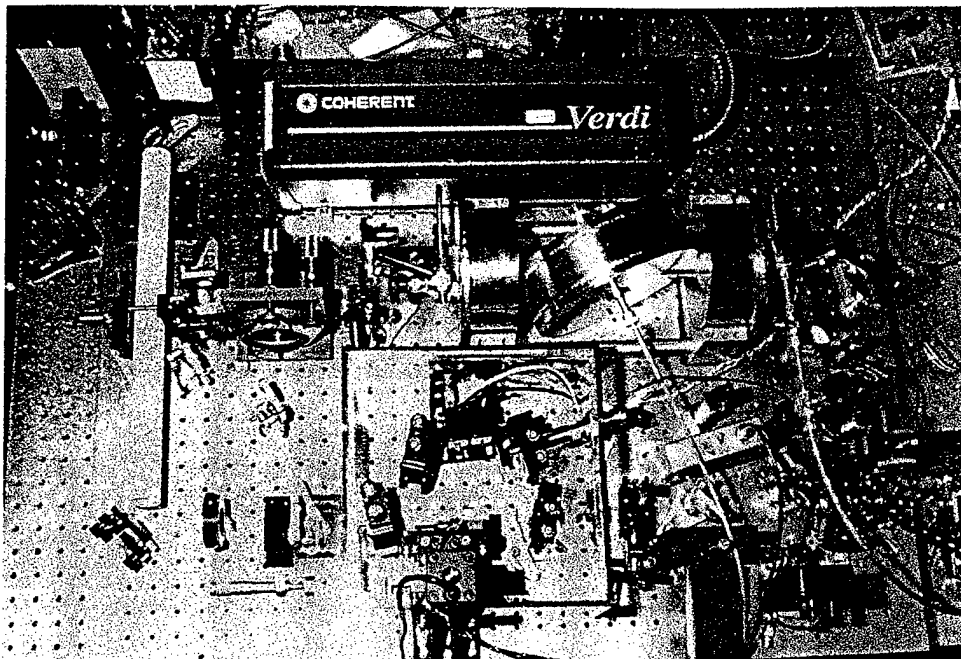


Figure 9. Photograph of the photoacoustic spectrometer showing major components such as the pump laser (top), photoacoustic cell (center) and the PPLN OPO at the bottom.

Although not shown in this figure 9, a Burleigh wavemeter was used to record the  $3\ \mu\text{m}$  light from the OPO. Ultimately, we hope to replace the wavemeter with a molecular calibration cell to obtain absolute wavelength measurements. Also not shown in the photograph were two lock-in amplifiers which were used to detect the microphone signal and to detect a fraction of the  $3\ \mu\text{m}$  light for normalization (ratioing) with the photoacoustic signal. It was necessary to ratio the photoacoustic signal with the normalization measurement since the OPO power could change while scanning. The analog output of the lock-in amplifiers were then fed directly into the computer.

All of the data analysis, acquisition and control was performed by LABView software running on the laptop computer. The interface between the computer, laser and photoacoustic cell was through a PC-MCIA card and a GPIB card installed inside the IBM laptop. These cards were about the size of a credit card and were extremely versatile as they had many input and output channels. At this point, most of the laser scanning control and data acquisition has been automated. The scanning etalon and PPLN stepper motor were controlled through the PC-MCIA card and the wavemeter was controlled through a GPIB interface.

## **Metals Emissions Monitoring Channel**

### **Introduction**

The second-half of the system is devoted to monitoring elemental composition in both gas and condensed phases employing the laser-induced breakdown (LIBS) or laser-induced plasma spectroscopy (LIPS) technique. The first LIPS experiment can be dated back to the early 70s. The LIBS or LIPS are established techniques for detection of elements in various media – soil, liquid, gas, and airborne particulate matter, although a unified theory of laser-induced breakdown and plasma formation has not been established in the literature to facilitate the design of the LIPS. Experiments have to be conducted to determine operational parameters under specific conditions. Research data on the use of LIPS on airborne particulate matter are limited, and some literature findings were even inconsistent. We have thus conducted a series of systematic studies over the year in an attempt to gather information to assist our design of the advanced LIPS system to be used for metal monitoring. To employ LIPS in the design of a continuous metals emission monitor (CEM) that is both sensitive and field portable, advances in laser and aerosol technologies, spectrometer, and digital signal processing are necessary.

The laser-induced breakdown and plasma spectroscopy is in essence an emission-based spectroscopy. A pulsed high-energy laser beam (approximately 120 mJ per pulse) was tightly focused onto a sample to create a focal volume of approximately  $10^{-8}$  cm<sup>3</sup>. The energy in this micro volume would reach a power density level on the order of 1,000 GW cm<sup>-2</sup> creating a plasma whose core temperature reaches 20,000°K or higher. All material inside this plasma volume would be vaporized; millions and billions of energetic ions and electrons would be produced due to violent energy-matter interaction in the plasma. Elemental atoms would release light at their characteristic wavelengths as they relax from the plasma-excited states, when the excitation laser energy disappeared in between pulses. A gated intensified detector can be used to collect the light for spectrochemical analysis to determine the identity and amount of the elements. Since the laser we used pulsed at 10 Hz, it means all the processes (breakdown, plasma ignition, triggering, gating, spectral-analysis, and data processing) need to be completed in a period of approximately 100 milliseconds. With such a high data-throughput rate, the LIPS system can be employed as a continuous metal monitor as long as the system can maintain its performance at extreme emission source conditions for a sustained period of time.

### **LIPS System**

The basic configuration of the LIPS is shown below in figure 10. A high-power pulsed (a dash line indicating pulsed light) Nd:YAG laser emitting 532-nm light was used

as the excitation source. The light was tightly focused to a small focal volume inside the sample cell to create a plasma spark. The emission light of the spark was collected and analyzed by a spectrometer that consists of a grating and intensified detector. When the laser fires, it also sends a trigger signal to a delay generator that postponed for a pre-selected time interval before it sends a second trigger signal to the spectrometer for emission light retrieval. The delay time was species dependent and can only be determined

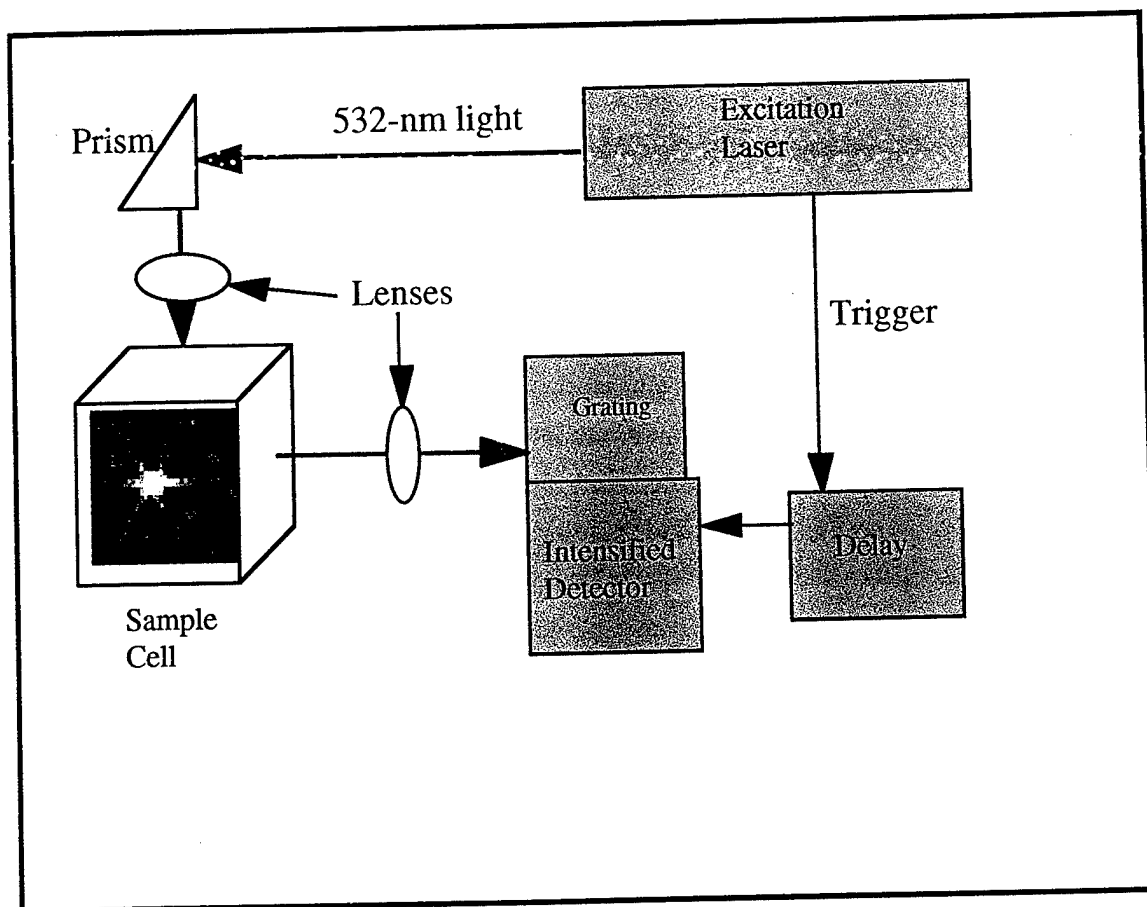


Figure 10. Schematic of the LIPS spectroscopy portion of the spectrometer.

experimentally. The pulse rate of the green (532-nm) laser was 10 Hz with a pulsewidth of 7 ns, and the nominal power intensity used was around 100-120 mJ per pulse. Using this energy deposition pattern, the efficiency of plasma formation was high (> 99%). The optical grating of the spectrograph was 1200 groves/mm that was coupled with a linear 1024 pixel intensified charge-coupled device (ICCD) detector to produce a spectral

resolution of approximately 0.05 nm. The trigger control, delay generation, grating and signal processing tasks were performed on a Pentium-266 MHz computer through a combination of PCI interfaces connecting RS 232 and GPIB devices. These functions have recently (October 1998) been successfully migrated to a Pentium 333 MHz laptop platform that is to be the LIPS control console during future field operations.

A number of laboratory experiments were conducted during the fiscal year 1998 (FY98) to improve the sensitivity of the spectroscopic system in detecting mercury and chromium and to optimize the system design configuration. Mercury is a ubiquitous element in the environment, and has been used widely in the industry from the dental application, coal burning for electricity generation and battery manufacturing to nuclear processing. Elemental mercury and mercury species (e.g., methyl mercury and mercuric chloride) are highly toxic to children's neurological functions. Mercury and mercury compounds are the top priority hazardous airborne metals among the other 14 to be regulated in the near future. Chromium is also a toxic element and an occupational hazard to chromium plating workers in some DoD and DOE facilities.

The accomplishments of FY98 included systematically examining the effects of laser power density, wavelength, and carrier gas on the detection of chromium and mercury in condensed phase using LIPS. Additionally, we were also ahead of the schedule for a fiscal year milestone in the employment of an aerosol beam-focusing module that was designed to improve the LIPS detection limit and sensitivity. Most of the results obtained in this fiscal year will be submitted for publications in peer-reviewed journals in the first quarter of FY99.

### **In-Situ Aerosol Measurements of Hg(o) and Cr Elements in Real Time**

Measurement of metals in airborne particulate matter has been exclusively done with filter sampling followed by laboratory analysis using techniques such as atomic absorption, inductively coupled plasma – mass spectroscopy, and X-ray fluorescence. Such a process is time-consuming, labor-intensive, and costly. The results are typically time-integrated over a period of several hours, and offer little use to emission monitoring and pollution control management. Within the scope of multi-element detection, ORNL has been focusing on the development of *in-situ* LIPS detection for elemental mercury and chromium in airborne particulate matter in real time virtually eliminating the sampling steps and producing no secondary analytical waste. The other hazardous air pollutants other than mercury and chromium that were on the EPA list will be examined as well during FY99. There has been no reliable commercial instrument for real-time, in-situ and portable multi-elemental measurement.

## In-Situ Real-Time Measurement of Hg

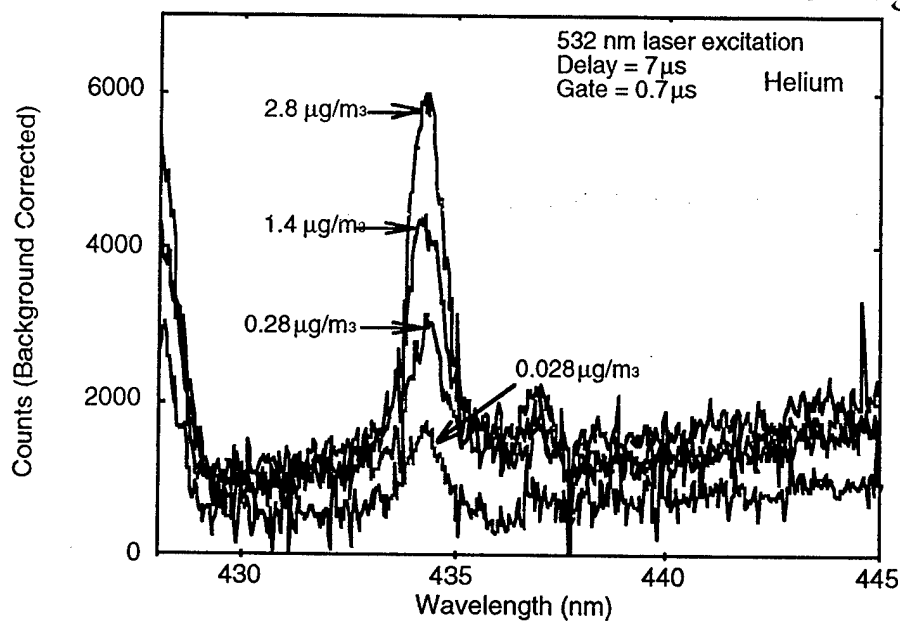


Figure 11. Real-time in-situ measurement of elemental mercury embedded in aerosol particles of median diameter of 0.3  $\mu$ m and number density of approximately  $10^6$  cm<sup>-3</sup>. Aerosol mercury concentrations ranged over two orders of magnitude from 28 ng m<sup>-3</sup> to 2.8  $\mu$ g m<sup>-3</sup>. The excitation wavelength was 532 nm and the carrier gas was helium.

## In-Situ Real-Time Measurement of Cr

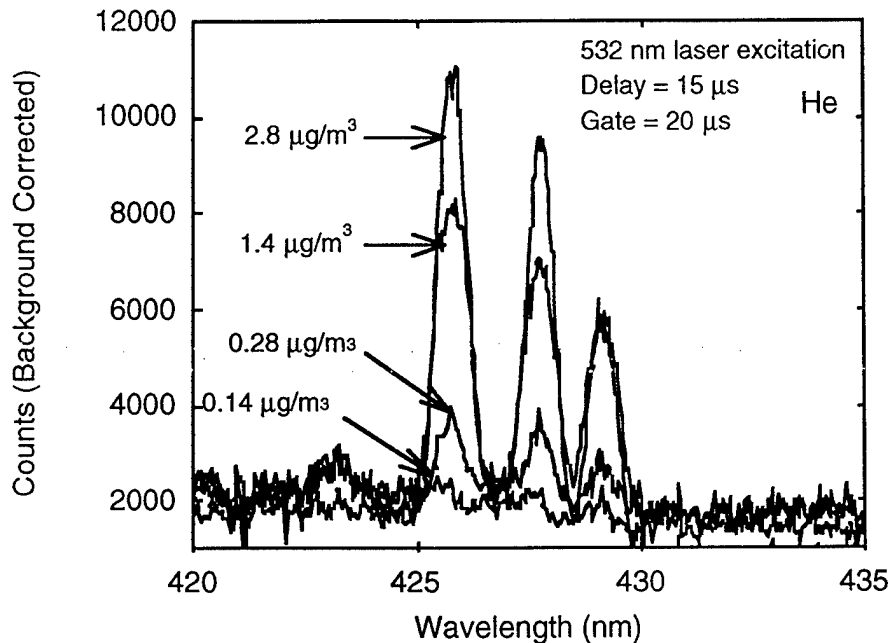


Figure 12. Real-time in-situ measurement of chromium embedded in aerosol particles of median diameter of  $0.3 \mu\text{m}$  and number density approximately  $10^6 \text{ cm}^{-3}$ . Aerosol mercury concentrations ranged over two orders of magnitude from  $140 \text{ ng m}^{-3}$  to  $2.8 \mu\text{g m}^{-3}$ . The excitation wavelength was 532 nm and the carrier gas was helium.

We have also conducted LIPS experiments using wavelengths of 1064 and 266 nm of the Nd:YAG laser in addition to 532 nm. We found that the 266-nm wavelength created a substantially higher noise background compared to that of 532-nm at a given elemental concentration, while similar observations were made also for the 1064-nm wavelength. Such a noise-to-signal ratio would require the use of high spectral resolution ( $\sim 0.01 \text{ nm}$ ) detector, which in turn will reduce the likelihood of real-time multi-elemental analysis capability. The multi-photon contribution to the plasma generation cascade by the 266-nm light appeared not working in favor of LIPS detection. Furthermore, much less 532-nm energy was required to create the plasma than by 1064-nm suggesting a possible use of smaller and less powerful laser that we will examine closely in FY99 using a Nd:YAG microchip laser.

Figures 11 and 12 above demonstrated real-time *in-situ* LIPS detection of mercury and chromium in aerosol phase and the feasibility of the technique as a continuous emission monitor for metal concentrations in condensed phase. The condensed phase presents the

greatest challenge to the US Environmental Protection Agency in regulating the airborne particulate matter (e.g., PM2.5). Being able to detect particle toxicity introduced by hazardous metals such as mercury and chromium using our LIPS technique, one would be able to further advance the health science and understand mortality issue caused by airborne PM2.5 particles. Better air pollution control strategies including emission reduction and engineering process control using the LIPS monitor can be designed.

The achieved minimal detection levels of aerosol elemental mercury (28 ng m<sup>-3</sup>) and chromium (140 ng m<sup>-3</sup>) were by no means optimal, and will be improved in FY99, but they were lower than most reported literature values. Noise reduction and rejection, auto-alignment of optical and aerosol beams, and signal processing would improve the sensitivity and reduce the instrument's detection limits of these two elements.

### **Effects of Carrier Gas**

The choice and effects of a carrier gas on the LIBS or LIPS measurement had been investigated by other LIPS researchers. The results were quite inconsistent. Some indicated that helium gas, for example, enhances the detection of some metals, while others pointed to a contradictory direction. The problem was however relevant to our work not only because it was of interest in advancing laser-induced plasma science, but it was important for us in using the *aerosol beam-focusing module*. If we have to use a third-body gas such as helium or argon, this requirement may complicate our design of a portable LIPS instrument. Therefore, it was considered worthwhile to examine the issue.

The delay time was defined as the elapsed time from the point when the plasma was formed. The target element shown in figure 13 was chromium that was embedded in the particles discussed earlier. Helium substantially cools the plasma as expected. However, the helium gas also dramatically compressed the operating window size as compared to the air at this particular wavelength. As shown in figure 13, the "usable" delay window was about 1 μs in size in the helium environment, while that window was 9 times longer in the air environment. The signal-to-noise (S/N) ratio was slightly higher in the helium environment; however, the gain of the LIPS sensitivity due to the increased S/N ratio did not justify the use of a consumptible such as helium.

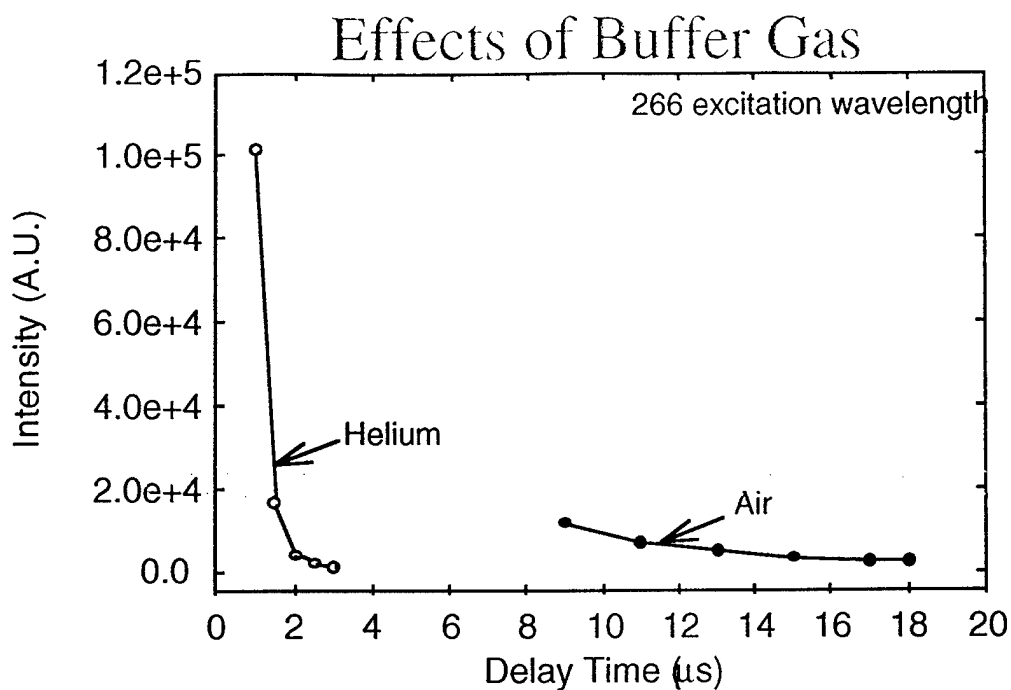


Figure 13. Plot of LIPS intensity at various delay times in the helium environment. Chromium particles.

#### Effect of Wavelength

We found that the delay time to optimal detection strongly depends on the excitation laser wavelengths. Using an exponential decay approximation, the 95% confidence intervals for the decay constants were [3.46, 3.73], [0.15, 0.25], and [0.08, 0.15]  $\mu\text{s}^{-1}$  in the same helium buffer gas. The greater the decay constants, the faster the plasma cools reducing the time-to-optimal-detection and the signal-to-noise ratio. The results indicate the 266-nm wavelength would not be a good choice for LIPS detection of chromium in the helium environment. On the other hand, helium enhanced the detection of mercury somewhat. The laser energy factor has not been normalized in the above discussion; thus, it is possible that the observations could potentially be attributed to the energy factor instead of wavelength. One of our ongoing tasks is to isolate the cause-effect relationship of the LIP-controlling parameters to reach a systematic understanding of the technique for use as a spectrochemical tool.

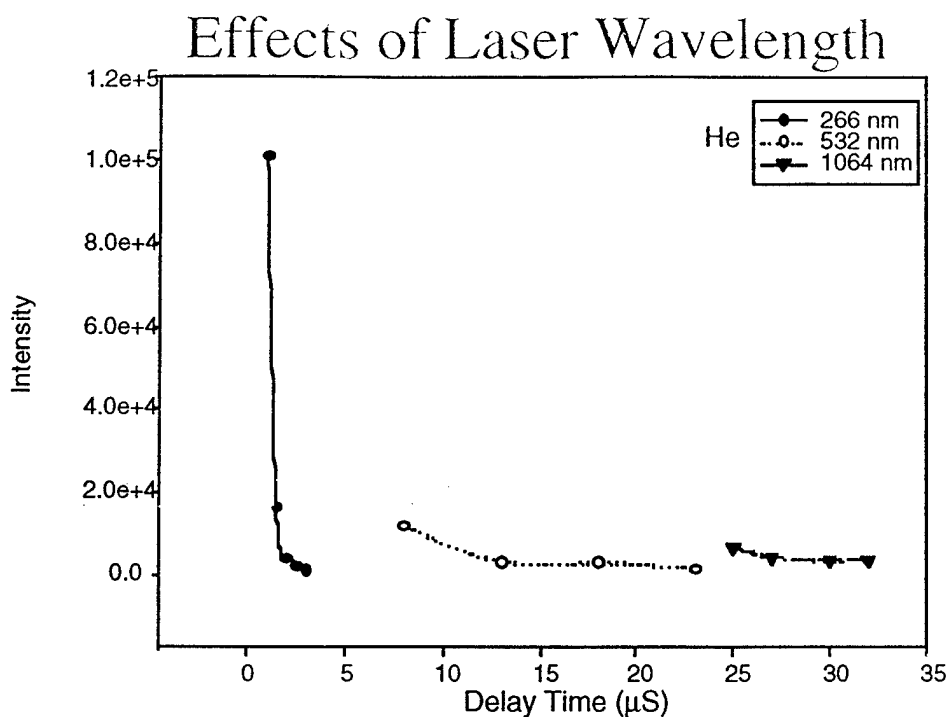


Figure 14. Plot of LIPS signal vs delay time using 3 different wavelengths.

#### Effects of Aerosol Beam-Focusing

One problem the LIPS technique encountered when it was used as a continuous emission monitor in previous field experiments was related to *in-situ* sampling. The spatial and temporal distributions of aerosol particles are random and inhomogeneous. Without a means to introduce material to the focal volume, the LIPS technique would suffer at least two folds of sampling uncertainty. One of which is related to the stochastic nature of aerosol distribution mentioned above, and the other is the “plasma efficiency” which the emission signal is effectively produced. By using an aerosol beam-focusing technique, we have increased the mass transfer efficiency of material to the plasma focal volume substantially and virtually eliminates the first sampling uncertainty.

## Effects of Aerosol Beam Focusing

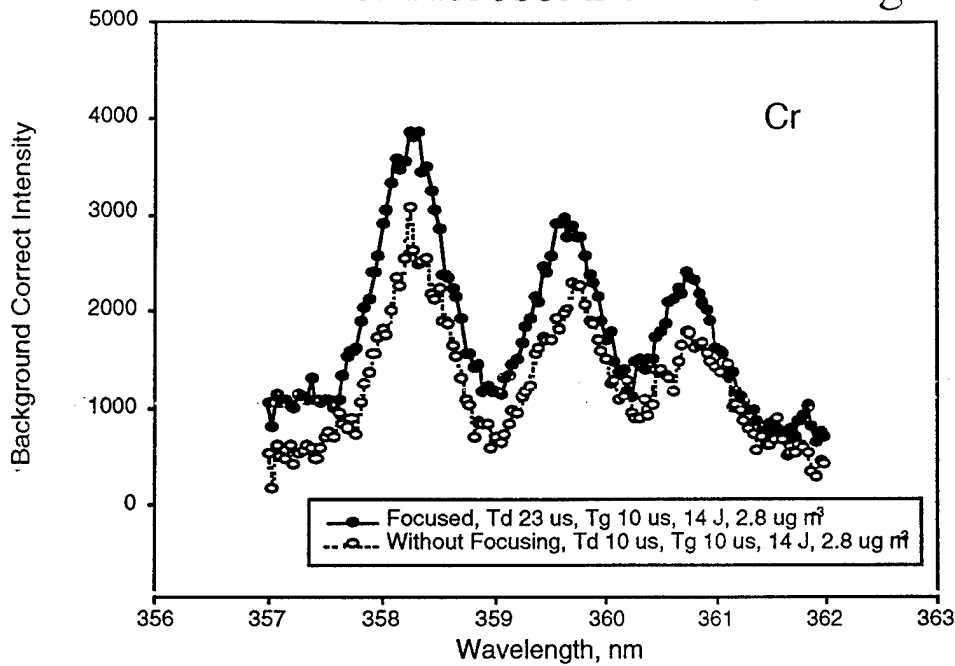


Figure 15. Plot of LIPS intensity as a function of wavelength obtained with and without the use of aerosol beam-focusing module.

As shown in the above figure, the improvement of the LIPS intensity was significant. At  $2.8 \mu\text{g m}^{-3}$  level, the single-stage sub-sonic flow aerosol beam-focusing module using helium as the carrier gas enhanced the LIPS signal. The enhancement was even more substantial at lower concentration levels. Focusing of particles leads to a great increase in mass transfer efficiency for LIPS detection that improves the detection sensitivity of aerosol chromium.

1. A. Balakrishnan, S. Sanders, S. DeMars, J. Webjorn, D. W. Nam, R. J. Lang, D. G. Meyhuys, R. G. Waarts, and D. F. Welch, *Opt. Lett.*, **21**, 952, (1996).
2. S. Sanders, R. J. Lang, L. E. Myers, M. M. Fejer, and R. L. Byer, *Electron. Lett.*, **32**, 218, (1996).
3. W. R. Bosenburg, A. Drobshoff, J. I. Alexander, L. E. Myers, and R. L. Byer, *Opt. Lett.*, **21**, 1336, (1996).
4. K. Schneider, P. Kramper, S. Schiller, and J. Mlynek, Conference on Lasers and Electro-Optics, Postdeadline paper CPD26, May 1997.
5. L. E. Myers, R. C. Eckardt, M. M. Fejer, R. L. Byer, W. R. Bosenburg, and J. W. Pierce, *J. Opt. Soc. Am. B*, **12**, 2102, (1995).
6. P. E. Powers, Thomas J. Kulp, and S. E. Bisson, "Continuous tuning of a CW periodically-poled lithium niobate optical parametric oscillator by use of a fan-out design," *Opt. Lett.*, **23**, 159-161 (1998)
7. D. D. Nelson, A. Schiffman, K. R. Lykke, and D. J. Nesbitt, *Chem. Phys. Lett.*, **153**, 105, (1988).
8. R. Gerlach and N. M. Amer, *Appl. Phys.* **23**, 319-326 (1980)
9. P. L. Meyer and M. W. Sigrist, *Rev. Sci. Instrum.* **61**, 1779-1807
10. F. Harren and Jorg Reuss, **Photoacoustic Spectroscopy** in *Encyclopedia of Applied Physics*, VCH Publishers, **19**, 413-435, (1997)
11. F. G. C. Bijnen, F. J. M. Harren, J. H. P. Hackstein, and J. Reuss, "Intracavity CO laser photoacoustic trace gas detection: cyclic CH<sub>4</sub>H<sub>2</sub>O and CO<sub>2</sub> emissions by cockroaches and scarab beetles," *Appl. Opt.* **35**, 5357-5367 (1996)